CAPTURE-NUMBERS AND ISLAND SIZE-DISTRIBUTIONS IN IRREVERSIBLE HOMOEPITAXIAL GROWTH

A Rate-Equation Approach

M. N. POPESCU[1], F. FAMILY
Department of Physics, Emory University, Atlanta, GA 30322

AND

J. G. AMAR
Department of Physics & Astronomy, University of Toledo, Toledo, OH 43606

Abstract. A fully self-consistent rate-equation approach to irreversible submonolayer growth is presented. This approach explicitly takes into account the correlation between the size of an island and the corresponding average capture zone. It is shown that this leads to capture numbers which depend explicitely on the island-size, and excellent agreement with experimental and Monte Carlo results is found for this size-dependency. Consequently, the predictions for the island-size distributions are in very good agreement with Monte Carlo simulation results over the whole range of coverages in the pre-coalescence regime.

1. Introduction

Molecular beam epitaxy (MBE) offers the possibility of atomic-scale controlled production of thin films, high quality crystals, and nanostructures [1]. In the submonolayer regime, the competition between nucleation, aggregation, and coalescence of islands leads to a distribution of islands of various sizes and morphologies which is experimentally measurable [2] and provides detailed information about the kinetics of growth. In the last three decades, considerable theoretical effort has been made toward understanding and predicting the island size-distribution [3, 4, 5, 6, 7, 11, 12].

One of the standard tools used in such theoretical studies of submonolayer growth is the rate-equation (RE) approach [3, 4, 13] which involves

[1] *present address*: Max-Planck-Institut für Metallforschung, Heisenbergstraße 1, D-70569 Stuttgart, Germany.

a set of deterministic, coupled reaction-diffusion equations describing the time (coverage) dependence of average quantities via a set of rate-coefficients usually called capture-numbers [3, 13]. The RE variables are the average densities of monomers, N_1, and of islands of size $s \geq 2$, N_s, where s is the number of atoms in the island. For irreversible growth, a general form of these equations may be written as,

$$\frac{dN_1}{d\theta} = \gamma - 2N_1 - 2R\sigma_1 N_1^2 - RN_1 \sum_{s\geq 2} \sigma_s N_s \tag{1}$$

$$\frac{dN_s}{d\theta} = RN_1 \left(\sigma_{s-1}N_{s-1} - \sigma_s N_s\right) + k_{s-1}N_{s-1} - k_s N_s, \quad \text{for } s \geq 2, \tag{2}$$

where θ is the coverage, γ is the fraction of the substrate not covered by islands, σ_s are the capture numbers, and k_s are the rates of deposition on top of existing islands. Here, the kinetic constant $R = D/F$ is the ratio of the diffusion constant D to the deposition flux F, where $D = D_h/4$ for the case of isotropic nearest-neighbor hopping with rate D_h on a two-dimensional isotropic square lattice (respectively $D = D_h/2$ in the one-dimensional case). The terms with σ_s describe the rate of monomer capture by other monomers or by existing islands, while the terms with k_s (where $k_s = s^{2/d_f}$ and d_f is the fractal dimension of the islands [7]) correspond to the deposition of adatoms directly on islands of size s.

While simple mean-field choices for the capture numbers lead to correct predictions for the scaling behavior of the island and monomer densities as a function of deposition flux and temperature [3, 5, 14], in order to make quantitative predictions more accurate expressions for the rate-coefficients should be used. Recently, Bales and Chrzan [7] have developed a self-consistent RE approach which leads to quantitative predictions for the average island and monomer densities in two-dimensional irreversible growth. Similar results have also been obtained for one-dimensional growth [12] as well as for reversible two-dimensional growth [8]. However, in all cases the island-size distributions N_s are not correctly predicted. The reason is that spatial and temporal correlations in the growth of islands [9, 10, 11] are neglected in these approaches.

In this work we present a novel calculation scheme which captures the essential correlations between the size of the island, the corresponding average capture zone, and the capture number. A second set of equations, coupled to the usual rate equations, is used to describe the evolution of the island-size dependent capture zones. The combined set of equations self-consistently leads to size- and coverage-dependent capture numbers $\sigma_s(\theta)$ in good agreement with experimental [10] and kinetic Monte-Carlo (KMC) simulation results [6]. Furthermore, numerical integration of the full rate-

equations with these capture numbers leads to island-size distributions in good agreement with KMC simulations.

2. Monomer Diffusion and Local Capture Numbers

In what follows we restrict the discussion to the case of two-dimensional growth, but we note that the approach may be extended to one-dimensional growth [15]. Two models extensively used in studies of submonolayer growth [5, 6] are considered: a *point-island* model and an *extended island* model. In the *point-island* model each island occupies just one lattice site (which physically corresponds to islands growing only in a direction perpendicular to the substrate), while in the *extended-island* model an island occupies a number of lattice sites equal to its size s. The fraction of the substrate not covered by islands is then given by $\gamma = 1 - \theta + N_1$ for extended islands and by $\gamma = 1 - N$ for point islands (where $N = \sum_{s\geq 2} N_s$ is the total island density).

In order to take into account the correlation between an island and its local capture zone, we consider the following model for the environment of an island. An island of size s is approximated by a circular region of radius $R_s = \rho\, s^{1/d_f}$, where ρ is a "geometrical" prefactor which accounts for the circular approximation of the island area while the fractal dimension d_f depends on the morphology of the island (here for extended islands we consider only the case of compact shapes, i.e. $d_f = 2$). The area surrounding the island is divided into an inner ($R_s < r < R_{ex}$) and an outer region ($R_{ex} < r < \infty$). The inner region corresponds to an "exclusion" zone in which only monomers can be found. The area of the exclusion zone A_{ex} is assumed to be proportional to the area A_V of the Voronoi polygon surrounding the island, i.e. $A_{ex} = \eta A_V$ where the factor η (typically larger than 1) is assumed to be the same for all islands. Accordingly, the radius of this zone is $R_{ex} = \sqrt{\eta}\ R_V$, where $R_V = \sqrt{A_V/\pi}$ is the "radius" of the Voronoi polygon. In the outer region, corresponding to $r > R_{ex}$, we assume a "smeared" uniform distribution of monomers and islands which is independent of the size of the central island, as in Ref. [7].

This geometry naturally leads to the definition of a mean-field "nucleation" length $\xi_1 = 1/\sqrt{2\sigma_1 N_1}$ and to that of a monomer "capture" length $\xi = 1/\sqrt{2\sigma_1 N_1 + \sum_{s\geq 2} \sigma_s N_s}$. In terms of these quantities, and defining $\alpha = \xi_1/\xi$, one can follow the steps described in details in [7, 16] to obtain the quasistatic diffusion equation satisfied by the local monomer density,

$$\nabla^2 n_1 \simeq \begin{cases} \xi_1^{-2}(n_1 - \alpha^2(N_1/\gamma)), & \text{for } R_s < r \leq R_{ex}, \\ \xi^{-2}(n_1 - N_1/\gamma), & \text{for } r > R_{ex}. \end{cases} \tag{3}$$

For the case of irreversible growth, the (isotropic) local monomer density $n_1(r)$ must vanish at the island edge and must also match the average local density (N_1/γ) far away from the island (the renormalized value N_1/γ is due to the fact that the average local monomer density is actually larger than the overall monomer density N_1 by a factor of $1/\gamma$). In addition, the interior and exterior solutions must match at the exclusion zone boundary. The general solution of Eq. (3) satisfying the boundary conditions above is given by,

$$n_1(r) = \begin{cases} N_1 \left[\alpha^2/\gamma + aI_0\left(r/\xi_1\right) + bK_0\left(r/\xi_1\right)\right] & \text{for } R_s < r \leq R_{ex}, \\ N_1 \left[1/\gamma + c\ K_0(r/\xi)\right] & \text{for } R_{ex} < r < \infty. \end{cases} \quad (4)$$

where the coefficients a, b, and c are determined by the boundary conditions at the island edge and at the exclusion zone.

Equating the *microscopic* flux of atoms $2\pi R_s D[dn_1/dr]_{r=R_s}$ at the edge of the island to the corresponding *macroscopic* RE-like term $DN_1\tilde{\sigma}_s(A_V)$, one obtains the local capture number, $\tilde{\sigma}_s(A_V)$,

$$\tilde{\sigma}_s(A_V) = \frac{2\pi R_s}{\xi_1}\left[aI_1\left(\frac{R_s}{\xi_1}\right) - bK_1\left(\frac{R_s}{\xi_1}\right)\right]. \quad (5)$$

The size-dependent capture numbers σ_s needed in the rate-equations are then computed by averaging the local capture numbers $\tilde{\sigma}_s(A_V)$, Eq. (5), over the distribution of Voronoi areas. Defining $G_s(\theta; A_V)$ as the number density of Voronoi areas of size A_V surrounding an island of size s at coverage θ, one can thus write,

$$\sigma_s(\theta) = \langle \tilde{\sigma}_s(A_V) \rangle_{G_s} \equiv \frac{\sum_{A_V} G_s(\theta; A_V)\ \tilde{\sigma}_s(A_V)}{\sum_{A_V} G_s(\theta; A_V)} \quad (6)$$

where $\langle \ldots \rangle_{G_s}$ denotes the average with respect to the distribution $G_s(\theta; A_V)$.

3. Voronoi Area Distribution Evolution Equations

In order to use Eq. (6) to compute the capture numbers, one has to determine the Voronoi-area distribution $G_s(\theta; A)$. Taking into account the change in the areas by nucleation and aggregation of islands, and ignoring for the moment the break-up of Voronoi areas when new islands are nucleated, one can write a general set of evolution equations for the functions $G_s(\theta; A)$ in the following form,

$$\frac{dG_2(\theta; A)}{d\theta} = (dN/d\theta)\ \delta(A - A_{av}) - RN_1\tilde{\sigma}_2(A)G_2(\theta; A), \quad (7)$$

$$\frac{dG_s(\theta; A)}{d\theta} = RN_1\ [\tilde{\sigma}_{s-1}(A)G_{s-1}(\theta; A) - \tilde{\sigma}_s(A)G_s(\theta; A)] \quad (s \geq 3). \quad (8)$$

The first term on the right side of (7) corresponds to nucleation of dimers while the remaining terms in (7) and (8) correspond to growth of islands via aggregation. It has been assumed that the Voronoi areas around the (new) dimers nucleated at coverage θ are equal to the average Voronoi area at that coverage, $A_{av} = 1/N$. The break-up of larger areas due to nucleation, neglected in (8), will be accounted for through a uniform rescaling to be justified *a posteriori*.

In principle, Eqs. (7) and (8) can be numerically integrated. However, if the local capture number $\tilde{\sigma}_s(A)$ has no explicit dependence on the island-size s (as in the case of point islands), then an analytic solution can be obtained. We therefore consider the mean-field approximation $\tilde{\sigma}_s(A) \simeq \tilde{\sigma}_S(A)$ (where $S = (\theta - N_1)/N$ is the average island size). After changing the coverage variable to $x_A = \int_{\theta_A}^{\theta} R\ N_1(\phi)\ \tilde{\sigma}_S(A)\ d\phi$ (where $1/N(\theta_A) = A$ defines θ_A), (7) and (8) can be solved in closed form [15],

$$G_s(x_A; A) = B_A\ x_A^{s-2}\ e^{-x_A}/(s-2)! \qquad (s \geq 2). \tag{9}$$

In the aggregation regime Eq. (9) corresponds to a sharply peaked distribution as a function of A whose peak position $\hat{A}_s$ satisfies

$$x_{\hat{A}_s} = s - 2, \tag{10}$$

and, along with (6), one can approximate $\sigma_s = \tilde{\sigma}_s(\hat{A}_s)$.

Because the effects of break-up of Voronoi cells due to nucleation have been neglected in (7) and (8), these areas must be rescaled so that the average Voronoi area is equal to $A_{av} = 1/N$ as described in detail in [15, 16] (in the case of extended islands additional geometrical corrections are included). Accordingly, the capture numbers are approximated by

$$\sigma_s = \tilde{\sigma}_s(A'_s), \tag{11}$$

where A'_s is the rescaled and corrected $\hat{A}_s$.

4. Self-Consistency (Closure) Conditions

Because of the coupling between the evolution of the capture-zones distribution and that of the island densities, the local monomer density and capture numbers must satisfy certain self-consistency conditions.

Since the parameters ρ and η are independent of the island size and Voronoi areas, it is reasonable to use an approximation in which the Voronoi areas surrounding islands of size s are replaced by their average values. Denoting the average Voronoi area corresponding to an island of size s at a given coverage θ by A_s, this leads to the approximation $\sigma_s = \tilde{\sigma}_s(A_s)$.

The definition of the capture length ξ then leads to the capture number self-consistency condition,

$$2\sigma_1 N_1 + \sum_{s\geq 2} N_s \tilde{\sigma}_s(A_s) = 1/\xi^2. \tag{12}$$

If $n_1^t(A_s)$ denotes the total number of monomers in a Voronoi area of size A_s surrounding an island of size s, then the self-consistency condition for the monomer density corresponds to the requirement that the total monomer density in the Voronoi polygons must be equal to the average monomer density N_1, i.e.

$$\sum_{s\geq 2} N_s \; n_1^t(A_s) = N_1. \tag{13}$$

The general Eqs. (12) and (13) can be solved at any given coverage θ for two of the three unknowns ξ, η and ρ, once the third is known and once the average Voronoi area A_s is known for all s [17]. The details are presented elsewhere [15, 16], and in here we just note that the value ρ is fixed ($\rho \simeq 0.3$ for extended islands, respectively $\rho \simeq 0.12$ for point islands) such that the monomer and total island density are correctly predicted.

5. Results

Before presenting the results, let us briefly review the essential steps in the calculations.
1) The functions $\xi(\theta)$, $\xi_1(\theta)$, and $\eta(\theta)$ are pre-calculated by using contracted RE for the monomer and for the total island density as described in detail in [15, 16].
2) The integration of the full rate-equations (1) and (2) starts at very low coverage θ_0, with initial conditions $N_1(\theta_0) = \theta_0$, and $N_s(\theta_0) = 0$ for $s \geq 2$. At low coverage, for which both the average island-size S and typical values of x_A are small, the average capture number $\sigma_{av} = (1/\xi^2 - 1/\xi_1^2)/N$ is used in the island-density rate-equations.
3) At coverages such that the average island-size S is sufficiently large (we chose as criterion $S \geq 10$) and the peak in the Voronoi-area distribution $G_s(\theta; A)$ is well-defined, the appropriate Voronoi-area evolution equation results for σ_s are used as follows.
4) At the current coverage, Eq.(10) is solved at every s for the corresponding $\hat{A}_s$ and the rescaled and corrected values A'_s are calculated.
5) The new capture numbers are obtained from $\sigma_s = \tilde{\sigma}_s(A'_s)$, i.e. Eq. (11), and a new integration step is performed.

The coupled evolution of the island densities and capture zones determines self-consistently the capture numbers. As we have mentioned, pre-

dicting the correct values of the capture numbers is crucial for calculation of the island size-distribution. It is thus important to see how our results compare with the measured capture numbers from KMC simulations [9] or experiments [10]. Fig. 1 shows the rate-equations results (lines) for the

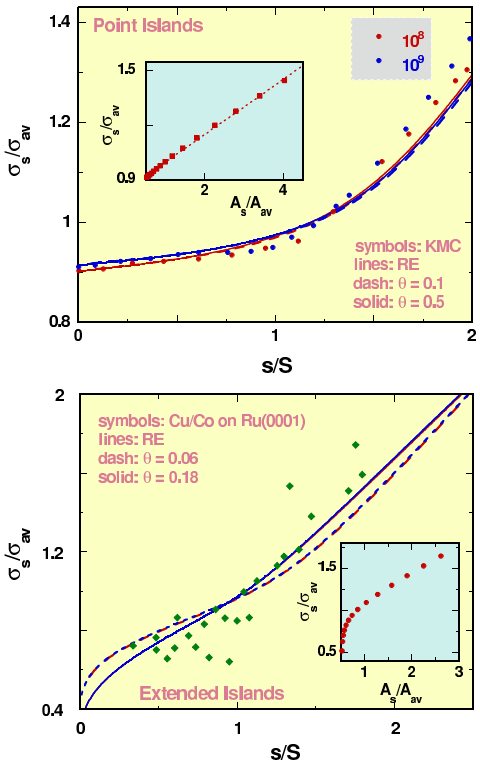

Figure 1. Scaled capture-number distributions σ_s/σ_{av} for point (top), respectively extended islands (bottom) as a function of the scaled island size (respectively, in insets, of the scaled average capture zone).

scaled capture number distribution σ_s/σ_{av} as a function of the scaled island-size for point (top) and extended (bottom) islands at $R_h = 10^8$ and 10^9 ($R_h = D_h/F$). In both cases it can be seen that the scaled capture-number distribution is essentially independent of coverage and weakly dependent on R_h, but depends strongly on the scaled island-size. Also shown are KMC simulation results (symbols) at $\theta = 0.2$ for $R_h = 10^8 - 10^9$ from Ref. [9] (top panel) and the *experimentally* measured capture number distribution for Cu/Co on Ru(0001) from Ref. [10](botom panel). As can be seen, there is good agreement with the simulations and experiments (within statistical fluctuations), although for large s/S the RE results are slightly below the measured distributions. Also, as shown by the insets, for $A_s/A_{av} > 1$ the

capture numbers are to a good approximation linearly dependent on the Voronoi areas, in agreeement with Ref.[9, 10].

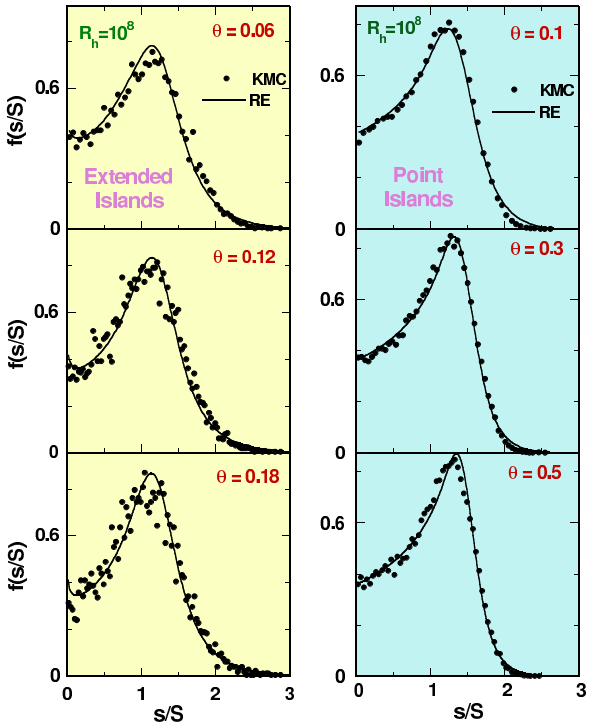

Figure 2. Scaled island-size distribution for extended (left), respectively point islands (right) calculated using RE's (solid lines), along with corresponding KMC results (symbols).

Since the size- and coverage-dependence of the capture number are correctly predicted by our approach, along with the average monomer and island densities (not shown), it is not surprising that the island size-distributions $f(s/S) = N_s S^2/\theta$ are also correctly predicted, as shown in Fig. 2 for $R_h = 10^8$. For both cases the agreement between the RE predictions and the corresponding kinetic Monte Carlo simulation results is very good. The dependence of the scaled island-size distribution on the island morphology is also clearly indicated: the peak is somewhat higher and shifted to the right for point islands in comparison with extended islands. A small "overshooting" of the peak value for extended islands and a slight shift in the peak position for point islands may be noted in our RE results, both being most probable caused by the fact that the uniform rescaling of

areas does not fully account for the neglect of the break-up in the area evolution equations. Similar results (not shown) have been obtained for other values R_h.

Our calculations may also be extended to the case of one-dimensional growth for which the capture zones are represented by the "gaps" between islands. For this case, as shown in detail elsewhere [15], the scaled capture

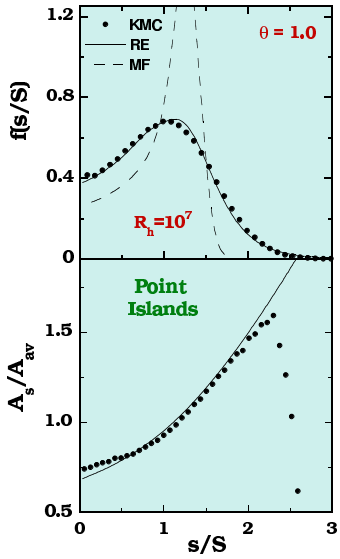

Figure 3. Scaled island-size distribution (top) for point-islands calculated using RE's (solid lines), along with KMC (symbols) and MF results (dashed lines); corresponding scaled average capture zone distribution (bottom).

numbers are basically equal to the scaled average capture zones. An example of results obtained for one-dimensional growth is shown for the case of point-islands in Fig. 3. As for the two-dimensional growth, there is very good agreeement between the predicted and the KMC measured scaled average capture zones (bottom panel), which indicates that the scaled capture rates are corectly predicted. As a consequence, the island size-distributions (top panel) obtained are in very good agreement with KMC results, in contrast with the typical "divergent" behavior (dashed line) obtained using the mean-field form $\sigma_s = \sigma_{av}$.

6. Summary and Discussion

We have presented a rate-equation theory of two-dimensional irreversible submonolayer growth in which the existence of a capture zone with a fluctuating area around every island and the correlations between its average

size and that of the island are explicitly taken into account. A general set of evolution equations for the Voronoi-area distributions has been solved analytically and the solution has been used to self-consistently determine the size- and coverage-dependent capture numbers $\sigma_s(\theta)$. The island-size dependence of the capture numbers was found to be in good agreement with simulation [9] and experimental [10] results. We note that the very good agreement found between the resulting scaled island-size distributions and KMC simulations suggests that the capture numbers σ_s depend essentially on the corresponding *average* capture zone, and not on the details of the capture zones distributions.

References

1. J.Y. Tsao, *Material Fundamentals of Molecular Beam Epitaxy, World Scientific*, Singapore, (1993).
2. J.A. Stroscio, D.T. Pierce, and R.A. Dragoset, *Phys. Rev. Lett.* **70**, 3615 (1993); J.A. Stroscio and D.T. Pierce, *Phys. Rev. B* **49**, 8522 (1994); D.D. Chambliss and R.J. Wilson, *J. Vac. Sci. Technol. B* **9**, 928 (1991); D.D. Chambliss and K.E. Johnson, *Phys. Rev. B* **50**, 5012 (1994); F. Tsui, J. Wellman, C. Uher, and R. Clarke, *Phys. Rev. Lett.* **76**, 3164 (1996).
3. J.A. Venables, G.D. Spiller, and M. Hanbucken, *Rep. Prog. Phys.* **47**, 399 (1984); J.A. Venables, *Philos. Mag.* **27**, 697 (1973); *Phys. Rev. B* **36**, 4153 (1987).
4. G. Zinsmeister, *Thin Solid Films* **2**, 497 (1968); *ibid* **4**, 363 (1969); *ibid* **7**, 51 (1971).
5. J.G. Amar, F. Family and P.M. Lam, *Phys. Rev. B* **50**, 8781 (1994); J.G. Amar and F. Family, *Phys. Rev. Lett.* **74**, 2066 (1995); J.G. Amar and F. Family, *Thin Solid Films* **272**, 208 (1996).
6. M.C. Bartelt and J.W.Evans, *Phys. Rev. B* **46**, 12675 (1992); M.C. Bartelt and J.W. Evans, *J. Vac. Sci. Tech. A* **12**, 1800 (1994).
7. G.S. Bales and D.C. Chrzan, *Phys. Rev. B* **50**, 6057 (1994).
8. G.S. Bales and A. Zangwill, *Phys. Rev. B* **55**, 1973 (1997); M.N. Popescu, J.G. Amar, and F. Family, *Phys. Rev. B* **58**, 1613 (1998).
9. M.C. Bartelt and J.W. Evans, *Phys. Rev. B* **54**, R17359 (1996).
10. M.C. Bartelt, A.K. Schmid, J.W. Evans, and R.Q. Hwang, *Phys. Rev. Lett.* **81**, 1901 (1998).
11. P.A. Mulheran and J.A. Blackman, *Philos. Mag. Lett.* **72**, 55 (1995).
12. J.A. Blackman and P.A. Mulheran, *Phys. Rev. B* **54**, 11681 (1996); P.A. Mulheran and J.A. Blackman, *Surf. Sci.* **376**, 403 (1997).
13. M. von Smoluchowski, *Z. Phys. Chem.* **17**, 557 (1916); *ibid* **92**, 129 (1917).
14. J.A. Blackman and A. Wilding, *Europhys. Lett.* **16** (1), 115 (1991); C. Ratsch, A. Zangwill, P. Smilauer, and D.D. Vvedensky, *Phys. Rev. Lett.* **72**, 3194 (1994).
15. J.G. Amar, M.N. Popescu, and F. Family, *Phys. Rev. Lett.* **86**, 3092 (2001); to appear in *Surface Science*.
16. M.N. Popescu, J.G. Amar, and F. Family, to appear in *Phys. Rev. B*.
17. The interpretation of the self-consistency conditions is one of the major differences between the one- and two-dimensional growth. Eq.(13) is identically satisfied in the case of one-dimensional growth, while Eq.(12) leads to corrections (due to spatial fluctuations) in the mean-field expression of the average capture number σ_{av}.